Optimization of Steel Arch Rib Lateral Bracing

Joseph Garth Eixenberger

A project report submitted to the faculty of
Brigham Young University
in partial fulfillment of the requirements for the degree of

Master of Science

Richard J. Balling, Chair
Fernando S. Fonseca
Paul W. Richards

Department of Civil and Environmental Engineering

Brigham Young University

June 2014

ABSTRACT

Optimization of Steel Arch Rib Lateral Bracing

Joseph Garth Eixenberger
Department of Civil and Environmental Engineering, BYU
Master of Science

This project examines the use of the stress design ratio to optimize the lateral bracing between arch ribs. Literature review on the design of bracing between arch ribs is given. Using the design processes set out, an excel worksheet was modified to account for the brace sizing throughout a long span arch bridge. These values were then checked against the actual design of the Lupu Bridge.

Keywords: stress design ratio, arch rib lateral bracing, Lupu Bridge.

TABLE OF CONTENTS

LIST OF TABLES

LIST OF FIGURES

1 INTRODUCTION

Arch bridges have been constructed since about 1300 BC, but it wasn't until the Roman Empire that they truly were utilized in a meaningful way. During that time those bridges were used to build roadways and aqueducts. Due to the nature of the arch bridge those structures were able to span longer distances than previous bridges with limited material use and last a long period of time. In fact many of the bridges built during that time are still in use today.

The arch bridge works by building the structure in such a way that the majority of it is in compression and the tension forces are negligible. This makes concrete and masonry great materials for construction as they are both strong in compression. However, due to the material properties, the span length of an arch was limited to about 40 meters. To overcome this limitation viaducts, or a bridge composed of several small spans, were used.

To span even greater distances in modern construction steel has replaced concrete and a truss style bridge is utilized instead of a solid structure. Using these methods spans up to 552 meters has been achieved. However, by using the trusses between arch ribs, it becomes more susceptible to out-of-plane buckling.

This project examined steel arch bridges for the out-of-plane buckling, and their need for lateral braces between the steel arch ribs. Research on the different loads that affect the lateral bracing was examined and are presented in this project report. An excel worksheet was created to optimize the amount of steel needed for these braces using the stress ratio method. These results were then compared with the actual design of the Lupu Bridge.

2 LITERATURE REVIEW

In preparation of carrying this project several articles and books were read on the design process for the lateral bracing between arch ribs. The following is a brief review of this literature.

2.1 **Out-of-Plane Buckling of Solid Rib Arches Braced with Transverse Bars**

In this article Tatsuro Sakimoto and Yoshio Namita explored a numerical analysis of the buckling load caused by the out-of-plane buckling in a solid circular arch rib bridge. Using the transfer matrix method general equations the out-of-plane buckling were derived dependent on the flexural rigidity of the arch ribs and the transverse bars, the number of transverse bars, and the end conditions of the arch ribs. The numerical analyses were then compared to results from a model test and were found to be within 90% of the experimental values. In addition to these results it was found that the number of transverse bars wasn't as important as the location of these braces.

2.2 **Ultimate Strength of Steel Arches Under Lateral Loads**

In this article Tatsuro Sakimoto and Sadao Komatsu explained the study of lateral braces in increasing the structural stability of an arch bridge to lateral loads. In the traditional design method lateral bracing is based on simple beam theory and treated independently of the design of the arch ribs. This article presented a method to design these systems together, and simplified numerical method to estimate forces on the lateral bracing. These methods and numerical analysis were designed and valid for a through type two-hinged, circular solid steel arch bridges of uniform depth. Model tests were done and compared to these numerical results. These test found that the proposed numerical analysis provide a conservative estimate of the combined vertical and lateral forces on the bridge. Surprisingly, the model tests also found that the shear force due to wind was almost double of conventional design methods.

2.3 **Numerical approach to the lateral buckling of steel tied-arch bridges**

In this article H. De Backer Outtier and Ph. Van Boaert discusses how finite element models of several steel tied-arch bridges were created and used to calculate the lateral buckling strength of steel tied-arch bridges. To model a more real world application several out-of-plane imperfections were included in the finite element model of the bridge. Based on the calculated values, the resistance to out-of-plane buckling was calculated. The results of the calculations were compared to the existing buckling curves for straight beams, which are generally used in the European Nations. From this comparison it was found that out-of-plane buckling of arches is less critical than when calculated using buckling curves from a straight beam as per the code in these nations. The article also elaborated in the lack of consensus on how to deal with the lateral buckling of arch bridges.

2.4 **Key Technology for Design of Lupu Bridge**

Yue Guiping details many of the design aspects of the Lupu Bridge in Shanghai. The design plans of the bridge are laid out and discussed. The key aspects of the design process of the bridge both for construction and operation of the bridge are discussed.

2.5 *Arch Bridges* from Steel Designer's Handbook

Arthur W. Hedgren, Jr. discusses many of the design aspects for steel arch bridges. Details on what needs to be considered for the design of the deck, arch rib, tie, hangers, deck lateral bracing, and rib lateral bracing are presented. Example designs are also provided using the LRFD design method.

2.6 *Arches* from Guide to Stability Design Criteria for Metal Structures

Ronald D. Ziemian presents the considerations for the structural design of arch for both in-plane and out-of-plane stability. For both types of stability design standards, structural analysis, and numerical methods are discussed. The differences that need to be considered for different type of arches are discussed and general design methods to account for these differences are given.

2.7 Arch Bridges

In this article Douglas A. Nettleton emphasizes aspects of arch bridge design such as wind stress analysis and deflection, stress amplification due to deflection, consideration of rib shortening moments, plate stiffening, and calculations for preliminary design. The article discusses the three major types of arches in use today, mainly steel, concrete, and covered arches. In the steel arch bridges a discussion is given on how to calculate the loads from winds as well as the preliminary design methods. Examples of the design methods are then given.

3 FORCES ACTING ON BRIDGE

In the design process it is first necessary to identify and estimate the forces acting on the structure. When designing lateral bracing in bridges two types of forces usually control the design: wind and seismic forces. However, these two forces are assumed to act separately. In general design practice this means that one type would be assumed to control and after designing against that type the other force would be checked. For this project only the wind force was considered and no check was done in regards to the seismic design. This decision was made as wind loads are generally considered to control in long span bridges (Barker, 2007).

In conjunction with the wind or seismic force it was also necessary to consider a nominal force that accounts for the buckling of the arch ribs, as well as the gravity force of the braces themselves.

3.1 Wind Loads

To estimate the wind loads the procedures in ASCE 7 were followed as stated in section 6.5.3. Usually a wind speed is estimated based on geographic location; for this project an assumed velocity of 178 mph was used. All other factors were assumed to be 1. Then a wind pressure, q, was found using the equation:

$$q = .00256 * k_z * k_{zt} * k_d * V^2 * I \qquad 3.1$$

Where V is the wind speed, I is the importance factor, k_z is the height factor, k_{zt} is the topographic factor, and k_d is the directionality factor.

Using this wind pressure acting on the rib was found at every brace point by multiplying this pressure by the depth of the arch rib and the average distance between brace points. A wind reduction coefficient was considered to account for truss style ribs compared to solid ribs.

To find how the wind forces act on the braces first the shear force on the arch rib is found by modeling the arch as a simply supported beam as shown in Figure 1. Where V1, V2, etc are the wind forces at the brace points. The shear force at any point along the arch rib is then the summation of all wind forces to the half-span point minus any of the wind forces up to that point.

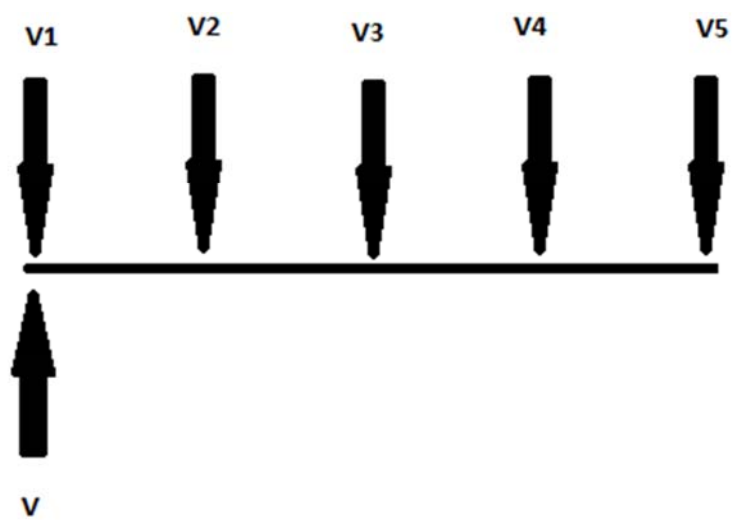

Figure 1 Shear Force Acting on Arch Rib

3.2 Buckling Load

The buckling load is an assumed nominal force that is estimated to deal with the arch ribs buckling. When an arch rib begins to buckle part of the vertical force from the rib, hangers, struts, and other components of the bridge then have a lateral component due to the deflection.

The best method to estimate this force is still under debate and dependent on the type of arch bridge (De Backer 2007).

Many methods have been developed to estimate the buckling load on the bracing between the arch ribs. These methods depend on the shape of the arch, parabolic or circular, the rib depth, the incline of the arch ribs, the type of arch, and the foundation conditions. Though this project mainly looked at the Lupu Bridge in comparison where one of the numeric methods could be utilized, the goal was to make the equations used be universal enough to be used on several bridges. Therefore, this project utilized the 2% rule, which states: "Bracing systems shall be proportioned to have strength perpendicular to the longitudinal axis of the braced member in the plane of buckling equal to 0.02 times the factored compressive force at each brace point in the member being braced, unless a detailed analysis is carried out…" (AASHTO 2012). Though this method can be universally applied to many bridges its major drawback is that it is considered highly conservative, and is usually not used in long span bridges as a more accurate load force can be found. The buckling force was then found using:

$$F_{buckling} = .02 * F_{comp} \qquad 3.2$$

Where $F_{buckling}$ is the buckling force and F_{comp} is the compressive force in the arch rib.

3.3 Gravity Load

The gravity load is to account for the self-weight of the brace. As the brace is secured between 2 arch ribs it is modeled as a fixed-fixed beam. The equation from the moment caused by gravity, M_{grav}, is then:

$$M_{grav} = \frac{A\gamma d^2}{12} \qquad 3.3$$

Where A is the area of the brace, γ is the density of steel, and d is the length of the brace.

4 BRACING TYPES AND ANALYSIS

Though there are many types of braces that can be utilized, this project concentrated on box girder braces. This was done as box girder braces are one of the most common brace types used in arch bridges and previous assumptions that exist in the excel worksheet could continue to be used. The brace is modeled as shown in Figure 2, where all the area of the brace is assumed to be in the four corners of the brace that are connected by webs of negligible size.

These braces are then considered to be laid out in two different patterns. The first pattern is vierendeel, or transverse bars, as shown in Figure 3. The second pattern is a diagonal truss that is also shown in Figure 3.

The depth of the brace is assumed to be a function of the arch rib depth. A reduction factor is multiplied by the arch rib depth to calculate the brace depth.

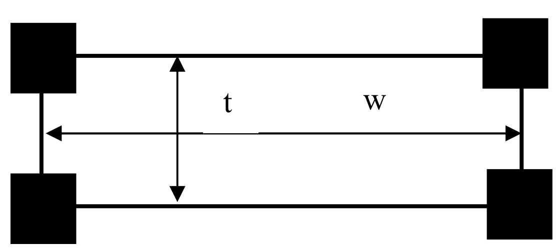

Figure 2 Brace Model

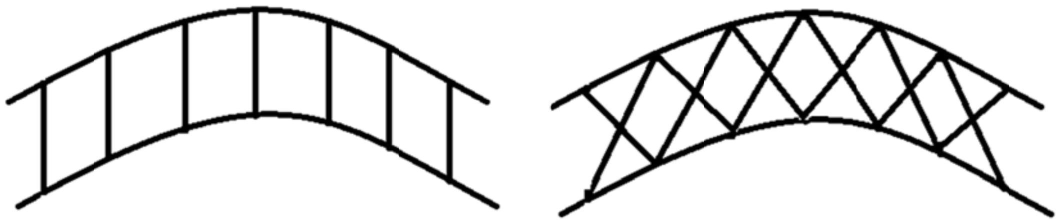

Figure 3 Vierendeel and Diagonal Bracing

4.1 Wind Force Acting on the Brace

Knowing the shear on the arch rib it is possible to solve for the force acting on the brace between arch ribs. From mechanics the force is:

$$F_{wind} = \tau s b \tag{4.1}$$

Where τ is the shear stress, s is the spacing between brace points, and b is the width of the brace. τ can be found using the shear formula:

$$\tau = \frac{VQ}{Ib} \tag{4.2}$$

Where V is the shear at any point, Q is the first moment of a plane area, I is the moment of inertia, and b is the width of the brace. The moment of inertia is solved using:

$$I = \frac{Ah^2}{2} \tag{4.3}$$

Where A is the area of the brace, and h is the distance between the two arch ribs. The first moment of a plane area is:

$$Q = \frac{Ah}{2} \tag{4.4}$$

Using these other values the shear stress can be written:

$$\tau = \frac{2VAh}{2Ah^2b} = \frac{V}{hb} \tag{4.5}$$

The force in the brace from the wind can then be written as:

$$F_{wind} = \tau s b = \frac{V}{hb} s b = \frac{Vs}{h} \tag{4.6}$$

This force is then used in determining the stress ratio but is used differently depending on the bracing pattern.

4.2 Vierendeel Bracing

The vierendeel bracing is treated like finding the stress in the web of an I-beam. The brace is modeled as shown in Figure 4. As the force from the wind acts on both ends of the brace in opposite directions a couple is created. To resist this couple a moment at the end of the brace is created and is calculated using:

$$M_{wind} = \frac{h}{2} * \frac{Vs}{h} = \frac{Vs}{2} \qquad 4.7$$

Where V is the shear force at that brace point, and s is the spacing between braces.

To optimize the brace, the stress ratio method is used. The stress ratio is solved using the following:

$$\sigma_{ratio} = \frac{\frac{F_{buckling}}{A} + \frac{M_{wind} + M_{grav}}{\frac{At}{2}}}{\sigma_{allow}} \qquad 4.8$$

Where A is the area of the brace, t is the depth of the brace, and σ_{allow} is the allowable stress.

The stress ratio is then multiplied by the original area to find the new area of the brace. This is continued until the stress ratio is equal to 1.

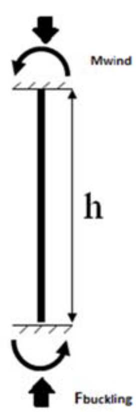

Figure 4 Vierendeel Model

4.3 Diagonal Bracing

The diagonal bracing is modeled as shown in Figure 5. The force in each member from the wind is then:

$$F_{wind} = \frac{Vs}{d} \qquad 4.9$$

Where V is the shear at that brace point, s is the spacing between braces, and d is the length of the brace.

To optimize the brace, the stress ratio method is used. The stress ratio is solved using the following:

$$\sigma_{ratio} = \frac{\frac{F_{buckling}+F_{wind}}{A}+\frac{M_{grav}}{\frac{At}{2}}}{\sigma_{allow}} \qquad 4.10$$

Where A is the area of the brace, t is the depth of the brace, and σ_{allow} is the allowable stress.

The stress ratio is then multiplied by the original area to find the new area of the brace. This is continued until the stress ratio is equal to 1.

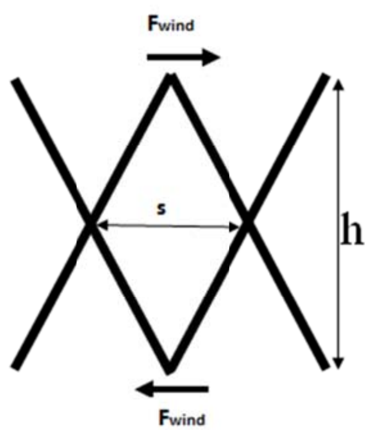

Figure 5 Diagonal Bracing Model

5 COMPARISON WITH LUPU BRIDGE

The Lupu Bridge is a steel arch bridge built in Shanghai, China. The main span of the bridge is 550 meters long and was the part of the bridge that was investigated. Using the modified spreadsheet values were compared to the actual design of the Lupu Bridge. Comparisons to several parts of the bridge are made to give an overall accuracy.

5.1 Design Values

All values that were used in the spreadsheet tried to reflect the actual values that were used in the design. Where actual values could not be found, best estimates were used. As the brace depth is roughly half of the depth of the arch rib, the brace/rib ratio was assumed to be 0.5. The other values used as well as the design layout are given in Appendix A.

5.2 Spreadsheet Values to Actual Values

The actual area of the arch rib, the force in each hanger, the force in the ties, and the max and minimum brace size areas were found and compared to the spreadsheets values (Guiping, 2008). A summary of the comparisons is shown in Table 1. Screenshots of the whole spreadsheet are given in Appendix B.

Table 1 Comparison of Actual Values to Spreadsheet Values

	Actual Value	Spreadsheet Value	Error (%)
Max Arch Rib Area (m^2)	2.2	1.97	10.5
Force in hanger (KN)	1245	1184.33	4.87
Force in tie (KN)	199280.32	203701.36	2.22
Max Brace Area (m^2)	0.24	0.203	15.4
Min Brace Area (m^2)	0.18	0.019	89.4

For the most part the values obtained from the spreadsheet area are fairly close to the actual values. However, there are some parts of the bridge that aren't accounted for that might explain the error. On the top of the arch ribs lies a viewing platform, as well as the lighting system over the bridge. The weight from these would increase the overall dead weight as well as live load put on to the arch ribs as well as the braces. As a check when a higher load is placed on the ribs the error decreases. The only area which is not impacted in any meaningful way is the minimum brace area. The high error here is most likely due to a minimum amount of steel that is required in the braces by code. No code reference to the minimum required area for braces was found and was therefore not included in the spreadsheet.

5.3 Conclusions

The modifications to the spreadsheet were successful in finding roughly the area of the maximum brace size. It was also successful in being able to be implemented to several types of bridges that will be investigated using the spreadsheet. However, it was unsuccessful in determining the minimum brace size. Further research on the minimum area of steel required would need to be investigated for the area of the bridge, as well as any other source of error.

REFERENCES

A. Outtier, H. De Backer and Ph. Van Bogaert. *Numerical approach to the lateral buckling of steel tied-arch bridge.* 5th International Conference on Arch Bridges, 2007.

American Association of State Highway and Transportation Officials. *AASHTO LRFD Bridge Design Specifications.* 2012

Barker, Richard and Jay Puckett. *Deisgn of Highway Bridges: An LRFD Approach*. New Jersey: John Wiley & Sons, 2007.

Guiping, Yue. *Key Technology Design of Lupu Bridge*. 2008.

Hedgren, Arthur. "Section 14 Arch Bridges". In *Structural Steel Designer's Handbook*. New York: McGraw-Hill Book Company, 2006.

Nettleton, Douglas. *Arch Bridges*. 2002.

Sakimoto, Tatsuro and Yoshio Namita. *Out-of-Plane Buckling of Solid Rib Arches Braced with Transverse Bars. 1971.*

Sakimoto, Tatsuro and Sadao Komatsu. *Ultimate Strength of Steel Arch Bridges Under Lateral Loads.* 1979.

Ziemian, Ronald. "Chapter 17 Arches". In *Guide to Stability Design Criteria of Metal Structures*. 6th edition. John Wiley & Sons, 2010.

APPENDIX A. DESIGN VALUES AND LAYOUT

High-Strength Wires				
allowable stress (KPa)	1180000			
density (KN/m^3)	77			
Structural Steel				
allowable stress (KPa)	247000		young's modulus (Kpa)	200000000
density (KN/m^3)	77			
Load Data				
wind pressure (KPa)	3.88			
wind pressure reduction coeff	1			
lane load (KN/m)	19.5			
number of lanes	7			
deck dead load (KPa)	3.59			
brace weight (Kpa)	1.00			
brace depth / rib depth	0.5			

There are 30 pairs of hangers spaced at 13.5 m intervals
http://www.bath.ac.uk/ace/uploads/StudentProjects/Bridgeconference2007/conference/mainpage/Ellis_Lupu.pdf

from plans assuming 2 struts on each side at 36.5 meters spacing

39.5 wide and 3m high bridge deck road surface is 28.7 m wide
http://www.arch-bridges.com/conf2008/pdf/431.pdf

deck is 46 meters above supports as shown in figure arch inclines at 5/1 slope so is 51 width at base and 11 m at top

The overall height of the web of arch rib has a transition from 9m at the skewback to 6m at the arch crown. http://www.arch-bridges.com/conf2008/pdf/431.pdf

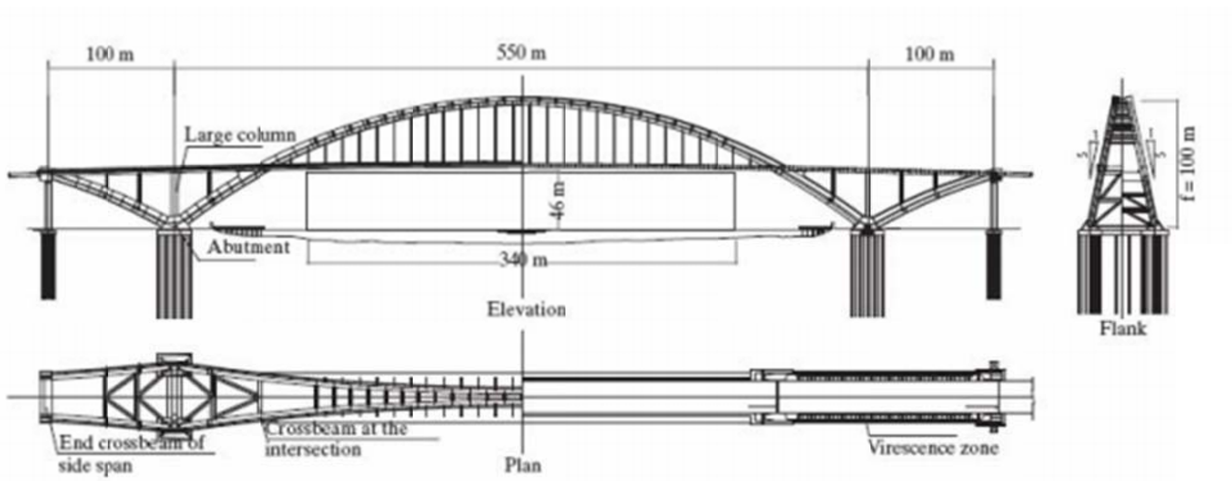
100 m
550 m
100 m
Large column
46 m
Abutment
340 m
Elevation
f = 100 m
Flank
End crossbeam of side span
Crossbeam at the intersection
Plan
Virescence zone

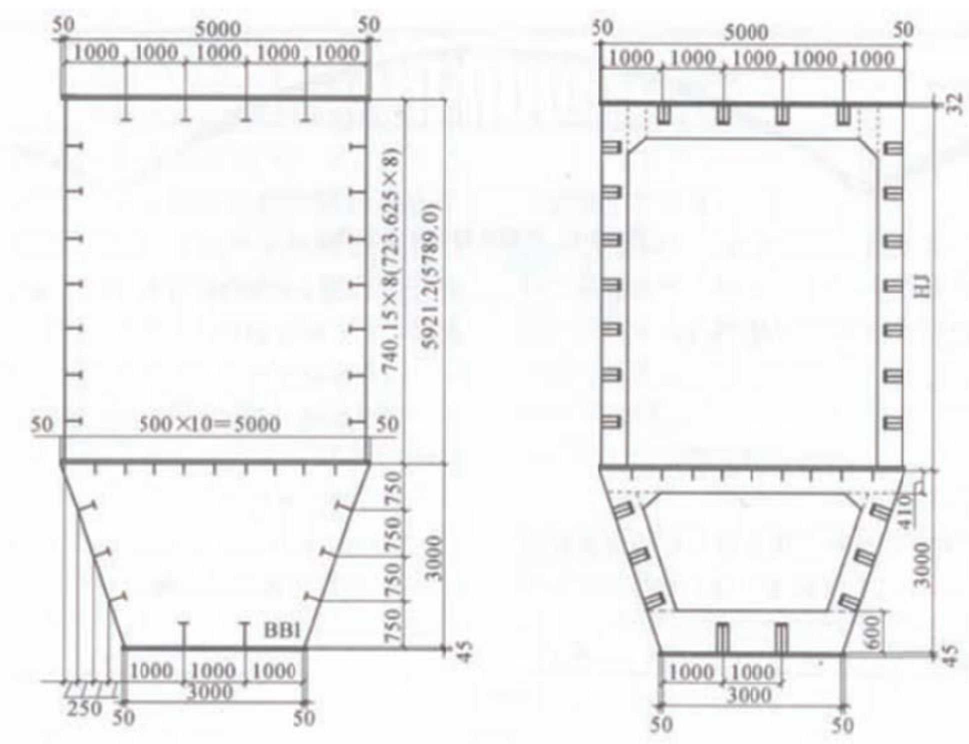
5000
1000 1000 1000 1000 1000
740.15×8(723.625×8)
5921.2(5789.0)
500×10=5000
750 750 750 750
3000
BB1
1000 1000 1000
3000
250
HJ
410
600
45
32

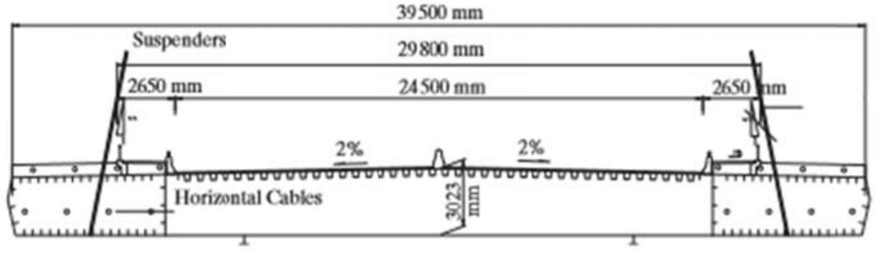
39500 mm
Suspenders
29800 mm
2650 mm
24500 mm
2650 mm
2%
2%
Horizontal Cables
3023 mm

APPENDIX B. SCREEN SHOTS OF SPREADSHEET

The actual spreadsheet is held by Dr. Balling, and can be accessed by request to him.

A26

	A	B	C	D	E	F	G	H
1	A deck	X space	X	w wind	M wind	w grav	M grav	deck
2	m^2	m	m	KN/m	KNm	KN/m	KNm	stress ratio
3	0.12874058	36.5	0	11.64	0	286.423025	47698.3843	1
4	0.16061957	36.5	36.5	11.64	109082.805	288.877707	48107.1656	1
5	0.18796659	36.5	73	11.64	202658.22	290.983427	48457.8338	1
6	0.0832285	13.5	86.5	11.64	233339.805	282.918595	6445.23923	1
7	0.09132455	13.5	100	11.64	261900	283.541991	6459.44098	1
8	0.09881925	13.5	113.5	11.64	288338.805	284.119082	6472.58784	1
9	0.10571259	13.5	127	11.64	312656.22	284.649869	6484.67984	1
10	0.11200457	13.5	140.5	11.64	334852.245	285.134352	6495.71696	1
11	0.1176952	13.5	154	11.64	354926.88	285.57253	6505.6992	1
12	0.12278446	13.5	167.5	11.64	372880.125	285.964404	6514.62657	1
13	0.12727237	13.5	181	11.64	388711.98	286.309973	6522.49906	1
14	0.13115892	13.5	194.5	11.64	402422.445	286.609237	6529.31668	1
15	0.13444412	13.5	208	11.64	414011.52	286.862197	6535.07942	1
16	0.13712795	13.5	221.5	11.64	423479.205	287.068852	6539.78729	1
17	0.13921043	13.5	235	11.64	430825.5	287.229203	6543.44029	1
18	0.14069155	13.5	248.5	11.64	436050.405	287.34325	6546.0384	1
19	0.14157132	13.5	262	11.64	439153.92	287.410991	6547.58165	1
20	0.14055956	13	275	11.64	440137.5	287.333086	6069.91144	1

	I	J	K	L	M	N	O	P
1	A' deck	A tie	A hang-strut	A rib	D hang-strut		Y hanger length	strut length
2	m^2	m^2	m^2	m^2	dm	m	m	m
3	0.12874058	0.82470188	0.05246188	0.99685013	1.82751727	0	0	46
4	0.16061957	0.82470188	0.05241901	1.43673025	1.82677035	24.7838044	0	21.2161956
5	0.18796659	0.82470188	0.05238348	1.68127489	1.82615119	46.0443031	0	0
6	0.0832285	0.82470188	0.00396329	1.76739414	0.50230478	53.0152133	4.01521327	0
7	0.09132455	0.82470188	0.00397042	1.83467036	0.50275654	59.50414	10.50414	0
8	0.09881925	0.82470188	0.00397702	1.88891817	0.50317438	65.5110833	16.5110833	0
9	0.10571259	0.82470188	0.00398309	1.92992963	0.50355838	71.0360431	22.0360431	0
10	0.11200457	0.82470188	0.00398864	1.9575712	0.50390863	76.0790195	27.0790195	0
11	0.1176952	0.82470188	0.00399365	1.97183732	0.5042252	80.6400124	31.6400124	0
12	0.12278446	0.82470188	0.00399813	1.97291873	0.50450814	84.7190218	35.7190218	0
13	0.12727237	0.82470188	0.00400209	1.96129047	0.50475752	88.3160478	39.3160478	0
14	0.13115892	0.82470188	0.00400551	1.9378279	0.50497338	91.4310904	42.4310904	0
15	0.13444412	0.82470188	0.0040084	1.90396457	0.50515577	94.0641495	45.0641495	0
16	0.13712795	0.82470188	0.00401077	1.86191765	0.50530473	96.2152252	47.2152252	0
17	0.13921043	0.82470188	0.0040126	1.81502965	0.50542028	97.8843174	48.8843174	0
18	0.14069155	0.82470188	0.00401391	1.76832633	0.50550245	99.0714261	50.0714261	0
19	0.14157132	0.82470188	0.00401468	1.72951056	0.50555125	99.7765514	50.7765514	0
20	0.14055956	0.82470188	0.00386513	1.71256119	0.49604578	100.000024	51.0000238	0
23			max area rib	1.97291873	m^2			
24		**Actual max area of rib**		**2.2**	**m^2**			

A26

	Q	R	S	T	U	V
1	rib depth	rib width	rib arc	V hang-strut	V grav	H grav
2	m	m	m	KN	KN	KN
3	9	51	22.0595045	12958.085	15776.3513	0
4	8.25648595	45.6909091	28.7098086	12947.4951	17435.3876	6363.91648
5	7.61867107	40.3818182	15.0844888	12938.7197	15500.6691	11315.4884
6	7.4095438	38.4181819	7.48926181	4676.67863	5983.61122	5175.8237
7	7.21487603	36.4545455	14.8773158	4685.09448	7329.15298	7329.15298
8	7.03466777	34.4909091	14.6814617	4692.88522	7334.63231	8324.80768
9	6.86891901	32.5272728	14.498989	4700.05084	7326.27961	9304.3751
10	6.71762975	30.5636364	14.3304087	4706.59136	7304.64599	10263.0276
11	6.5808	28.6000001	14.1762158	4712.50676	7270.34226	11196.3271
12	6.45842975	26.6363637	14.0368841	4717.79705	7224.09823	12100.3645
13	6.35051901	24.6727274	13.9128597	4722.46223	7166.84168	12971.9834
14	6.25706777	22.709091	13.8045546	4726.5023	7099.80672	13809.1241
15	6.17807603	20.7454546	13.712341	4729.91726	7024.68749	14611.35
16	6.1135438	18.7818183	13.6365449	4732.70711	6943.86575	15380.6626
17	6.06347107	16.8181819	13.577441	4734.87185	6860.76599	16122.8001
18	6.02785785	14.8545456	13.5352477	4736.41147	6780.44601	16849.4083
19	6.00670413	12.8909092	13.2601615	4737.32599	6674.1479	17486.2675
20	6	11.0000001	6.50096031	4560.8567	5489.63077	15096.4846
22					152525.363	203701.364
23		there are 4 hangers per point				**199280.3**
24		so max force per hanger is		1184.3315	KN	
25		**actual force in cable**		**1245**	**KN**	

	W	X	Y	Z	AA	AB	AC
1	sum V grav	sum X*V grav	M grav	F grav	V wind	sum V wind	sum X*V wind
2	KN	KNm	KNm	KN	KN	KN	KNm
3	0	0.00	0	246221.982	770.317898	0	0
4	15776.3513	0.00	57155.84	246221.982	919.723471	770.317898	0
5	33211.7389	636391.65	33001.16	235738.219	445.904183	1690.04137	33569.9067
6	48712.408	1767940.49	51510.18	229255.138	215.309012	2135.94555	66120.912
7	54696.0192	2285522.86	52617.27	226010.792	416.471398	2351.25456	84745.1416
8	62025.1722	3018438.16	54487.23	222956.545	400.723316	2767.72596	126392.281
9	69359.8045	3850918.93	57194.05	220100.31	386.418439	3168.44928	171874.378
10	76686.0841	4781356.44	60624.95	217449.889	373.513553	3554.86772	220949.52
11	83990.7301	5807659.20	64487.89	215012.895	361.968462	3928.38127	273428.174
12	91261.0723	6927291.91	68319.76	212796.66	351.746172	4290.34973	329171.317
13	98485.1706	8137328.36	71496.26	210808.146	342.813053	4642.0959	388088.801
14	105652.012	9434526.70	73244.45	209053.853	335.139011	4984.90896	450137.963
15	112751.819	10815439.11	72659.34	207539.719	328.697635	5320.04797	515322.501
16	119776.506	12276574.11	68726.82	206271.033	323.466346	5648.7456	583691.609
17	126720.372	13814640.37	60355.80	205252.347	319.426514	5972.21195	655339.405
18	133581.138	15426920.38	46424.44	204487.396	316.563571	6291.63846	730404.635
19	140361.584	17111861.21	25848.41	203979.037	309.041483	6608.20203	809070.683
20	147035.732	18860487.96	4.84	203731.459	151.342356	6917.24352	890039.551
22					7068.58587		
23	**Actual force in ties (KN)**						

A26

	AD	AE	AF	AG	AH	AI	AJ	AK	AL	AM	AN
1	M wind	alpha	beta	w live	M live	tie	hang-strut	rib	A' tie	A' hang-strut	A' rib
2	KNm			KN/m	KNm	stress ratio	stress ratio	stress ratio	m^2	m^2	m^2
3	0	0	0.32779071	136.5	0	1	1	1	0.82470188	0.05246188	0.99685013
4	229886.781	0.06636364	0.34911802	136.5	349838.128	1	1	1	0.82470188	0.05241901	1.43673025
5	426203.655	0.13272727	0.37375226	136.5	570504.207	1	1	1	0.82470188	0.05238348	1.68127489
6	492794.3	0.15727273	0.38387464	136.5	621413.441	1	1	1	0.82470188	0.00396329	1.76739414
7	556478.272	0.18181818	0.39463011	136.5	656687.317	1	1	1	0.82470188	0.00397042	1.83467036
8	614539.881	0.20636364	0.40608635	136.5	677017.455	1	1	1	0.82470188	0.00397702	1.88891817
9	667191.725	0.23090909	0.41832193	136.5	683168.205	1	1	1	0.82470188	0.00398309	1.92992963
10	714626.92	0.25545455	0.43142888	136.5	675986.608	1	1	1	0.82470188	0.00398864	1.9575712
11	757019.683	0.28	0.44551595	136.5	656414.022	1	1	1	0.82470188	0.00399365	1.97183732
12	794525.87	0.30454545	0.46071296	136.5	625499.773	1	1	1	0.82470188	0.00399813	1.97291873
13	827283.485	0.32909091	0.47717682	136.5	584417.213	1	1	1	0.82470188	0.00400209	1.96129047
14	855413.123	0.35363636	0.49509988	136.5	534482.689	1	1	1	0.82470188	0.00400551	1.9378279
15	879018.385	0.37818182	0.51472191	136.5	477178.008	1	1	1	0.82470188	0.0040084	1.90396457
16	898186.229	0.40272727	0.53634803	136.5	414177.118	1	1	1	0.82470188	0.00401077	1.86191765
17	912987.277	0.42727273	0.5603765	136.5	347377.817	1	1	1	0.82470188	0.0040126	1.81502965
18	923476.067	0.45181818	0.58734431	136.5	278939.387	1	1	1	0.82470188	0.00401391	1.76832633
19	929691.249	0.47636364	0.61800718	136.5	211327.041	1	1	1	0.82470188	0.00401468	1.72951056
20	931658.699	0.5	0.65207471	136.5	149631.162	1	1	1	0.82470188	0.00386513	1.71256119
21											

G32

	A	B	C	D	E	F	G	H	I	J	K	L	M	N	O
1	S wind	F nominal	A vieren	M wind vieren	M grav vieren	vieren	A' vieren	W vieren	A diag	d diag	F wind diag	M grav diag	diag	A' daig	W diag
2	KN	KN	m^2	KNm	KNm	stress ratio	m^2	KPa	m^2	m	KN	KNm	stress ratio	m^2	KPa
3									0.03407491	67.43505735	0	1491.4439	0.078757646	0.00268366	0.157269769
4	6298.267975	4924.439634	0.202592924	90411.03416	2713.896935	1	0.202592924	0.54	0.033816702	53.96213753	7438.416292	947.7859723	1.535071124	0.051911043	0.10711518
5	5378.544504	4714.764374	0.107711968	40566.29717	1127.055183	1	0.107711968	0.55	1.033816702	43.10722729	5741.547822	18490.32144	0.078966107	0.081636481	5.633365016
6	4932.640321	4585.10276	0.060178948	18470.9174	569.938093	1	0.060178948	0.62	2.033816702	39.14135588	5025.491079	29990.53956	0.05135996	0.104456744	21.30406994
7	4717.331309	4520.215848	0.098958071	35090.61384	843.8477105	1	0.098958071	0.51	3.033816702	39.37344808	5095.04636	45268.59072	0.046323479	0.140536944	16.95927342
8	4300.85991	4459.130899	0.092355957	31571.45493	704.991171	1	0.092355957	0.48	4.033816702	37.48557229	4674.28082	54556.33521	0.040301817	0.162570144	22.99307698
9	3900.136595	4402.006192	0.085855602	28274.01882	582.8723047	1	0.085855602	0.46	5.033816702	35.61241577	4270.056297	61447.04547	0.035753909	0.179978627	29.26875067
10	3513.718156	4348.997784	0.079448852	25176.50854	476.2194781	1	0.079448852	0.43	6.033816702	33.75642878	3880.774362	66176.81182	0.031961984	0.192852754	35.80764281
11	3140.204603	4300.257901	0.073128238	22258.10903	383.8191647	1	0.073128238	0.40	7.033816702	31.92060617	3504.798397	68981.72409	0.02862639	0.201352783	42.64091862
12	2778.23614	4255.933197	0.066886968	19498.88935	304.5095091	1	0.066886968	0.37	8.033816702	30.10863642	3140.402449	70097.87161	0.025605903	0.205713131	49.81476441
13	2426.489968	4216.162925	0.060718904	16879.70719	237.174352	1	0.060718904	0.34	9.033816702	28.32509733	2785.689784	69761.34326	0.022830283	0.206244593	57.39840794
14	2083.676915	4181.077053	0.054618525	14382.11588	180.7377806	1	0.054618525	0.30	10.0338167	26.57571338	2438.459579	68208.22749	0.020264869	0.20333398	65.49673786
15	1748.537904	4150.794371	0.048580862	11988.27401	134.1592466	1	0.048580862	0.27	11.0338167	24.86769358	2095.982256	65674.61235	0.017894144	0.197440705	74.27068605
16	1419.840269	4125.420654	0.042601429	9680.857826	96.42927773	1	0.042601429	0.24	12.0338167	23.21017139	1754.608393	62396.58558	0.015713202	0.189089793	83.97122368
17	1096.373924	4105.046931	0.036676124	7442.976158	66.56577747	1	0.036676124	0.21	13.0338167	21.61476691	1409.062342	58610.2347	0.013722816	0.178860674	94.99831868
18	776.9474099	4089.747928	0.03080113	5258.087827	43.61088211	1	0.03080113	0.18	14.0338167	20.09627962	1051.109395	54551.64709	0.011926238	0.167370639	108.0081709
19	460.383839	4079.580738	0.024817218	3052.382024	26.46242697	1	0.024817218	0.14	15.0338167	18.49344269	660.4718105	49488.6402	0.01015138	0.152613993	125.2406692
20	151.3423561	4074.629183	0.019192215	983.8706502	14.90115577	1	0.019192215	0.23	16.0338167	12.77742101	175.7968162	25195.56272	0.005314544	0.08521242	220.5975271
21						min brace area	0.019								
22					actual min brace area		0.180								
23						max brace area	0.203	m^2							
24					**actual max brace area**		**0.240**	m^2							
25															
26							max weight	0.62						max weight	220.5975271
27							average weig	0.37						average weig	58.59266601
28															
29															

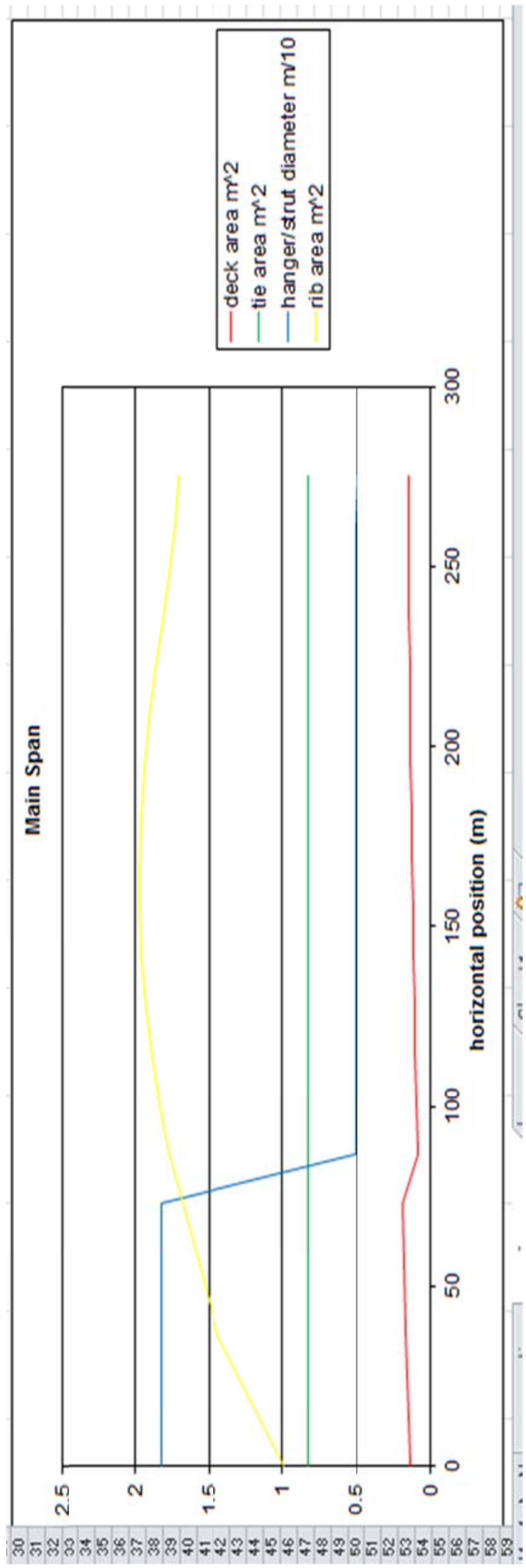
Main Span
deck area m^2
tie area m^2
hanger/strut diameter m/10
rib area m^2
horizontal position (m)